JOURNAL OF APPLIED PHYSICS **98**, 093708 (2005)

Deep donor-acceptor pair recombination in InGaAs-based heterostructures grown on InP substrates

T. H. Gfroerer,[a] C. E. Gillespie, and J. P. Campbell
Department of Physics, Davidson College, Davidson, North Carolina 28035

M. W. Wanlass
National Renewable Energy Laboratory, Golden, Colorado 80401

(Received 28 April 2005; accepted 28 September 2005; published online 7 November 2005)

We are investigating a series of lattice-matched $In_xGa_{1-x}As/InAs_yP_{1-y}$ double heterostructures with indium concentrations ranging between $x=0.53$ and $x=0.78$. The double heterostructures incorporating indium-rich alloys ($x>0.53$) experience lattice mismatch relative to the InP substrate. Previous work has produced convincing but indirect evidence that the distribution of defect levels in the $In_xGa_{1-x}As$ changes dramatically when the epistructure deviates from the lattice-matched condition. In particular, deep midgap states appear to give way to shallower near-band-edge states with increasing mismatch. Here, we report sub-band-gap photoluminescence measurements that explore these changes directly. We observe a broad low-energy peak in the spectra of the lattice-matched and nearly lattice-matched epistructures that is not present in the more mismatched case. The sub-band-gap emission blueshifts and grows superlinearly with photoexcitation up to and exceeding $1000\ W/cm^2$. This unusual behavior is attributed to transitions between ordinary acceptor levels and deep, defect-related donorlike states. We find no evidence for the shallower defect states that we expected to arise with increasing lattice mismatch. © *2005 American Institute of Physics*. [DOI: 10.1063/1.2126153]

I. INTRODUCTION

As materials scientists seek to extend the operating range of semiconductor devices, they are looking beyond simple pseudomorphic systems to structures that may incorporate significant lattice mismatch between epilayers and the substrate. Historically, these structures were likely to contain a high density of defects, which produce new energy levels in the forbidden gap of the semiconductor. And these localized defect states can act as carrier traps or recombination centers, impairing the performance of semiconductor devices. Yet previous experiments on the InGaAs-based heterostructures described in this report reveal a special feature of lattice mismatch in this material system. While the increasing mismatch relative to the substrate is expected to generate larger defect densities, which usually augment the detrimental nonradiative process, we find that the overall rate of defect-related recombination in the active layer of the mismatched epistructures shows little change from the nominally lattice-matched (LM) case.[1] In addition, photovoltaic devices that depend on severely mismatched InGaAs can perform exceptionally well.[2] These results are at least partly due to the presence of a carefully designed buffer between the substrate and the heterostructure, which reduces the dislocation density in the InGaAs.[2] However, we have also found evidence that the defect states themselves change with mismatch,[3] and these changes may contribute to the highly desirable outcomes noted above. Hence, we are investigating what distinguishes these states from the nonradiative centers that are typically found in mismatched epistructures.

Excitation-dependent radiative efficiency measurements indicate that the defect-related density of states (DOS) in the active layer of the lattice-mismatched epistructures is fundamentally different from that of the LM system.[3] A simple defect recombination model assuming defect levels concentrated near the middle of the band gap fits well in the LM case but the model does not fit the experimental results for the mismatched structures. In this latter case, we find that a redistribution of defect levels toward the band edges is required to obtain good fits. This analysis was later supported by fundamental differences in the temperature dependence of defect-related recombination in these structures.[4] We note that shallow states are more likely to act only as *temporary* carrier traps and are less likely to facilitate more detrimental nonradiative recombination.

If defect states within the forbidden gap are radiative, they may be observed with sub-band-gap photoluminescence (PL) measurements. For example, a broad PL peak approximately 100 meV below the band-to-band (B-B) emission has been observed in InGaAs epilayers nearly LM to InP.[5] The intensity of the peak showed a strong correlation with proximity to the interface region and degree of mismatch. A similar PL peak has been observed by others and a review of this work has been given by Bacher.[6] Bacher concludes that the sub-band-gap (SBG) emission is not related to an impurity and that imperfect arsenic incorporation may be involved. In the present work, we use SBG PL to obtain a direct check on the modified DOS interpretation[3] of our radiative efficiency results. It is important to note that recombination through deep levels is often predominantly nonradiative and PL from these states may be relatively weak. For example, deep levels are effective stepping stones for multiphonon transitions,

[a]Electronic mail: tigfroerer@davidson.edu

 © 2005 American Institute of Physics

Downloaded 07 Nov 2005 to 152.42.169.207. Redistribution subject to AIP license or copyright, see http://jap.aip.org/jap/copyright.jsp

which are frequently nonradiative. The large ionization energy associated with deep states means that a strong potential exists which localizes the carrier wave function near the defect site. Localization in real space implies delocalization in k space, which allows the carrier to couple more readily with phonons.

II. EXPERIMENT AND RESULTS

The LM $In_xGa_{1-x}As/InAs_yP_{1-y}$ double heterostructures are grown by atmospheric-pressure metal-organic vapor-phase epitaxy (MOVPE) on InP substrates. Indium concentrations in the unintentionally doped InGaAs layer, with an estimated background carrier density of approximately 1×10^{15} cm^{-3} n-type, vary from the LM condition ($x=0.53$) to severe mismatch ($x \approx 0.78$). The InAsP barriers adjacent and LM to the active InGaAs layer passivate the interfaces and confine carriers in the InGaAs. For $x > 0.53$, a buffer of InAsP compositional step-grading layers is incorporated between the InP substrate and the double heterostructure (DH) to accommodate the lattice mismatch. The abrupt steps in composition reduce the density of misfit dislocations in the DH by blocking or diverting upward-propagating threading dislocations and precluding their entry into the active region of the structure.[2] Further details on the sample structure are given in Ref. 4. Samples are mounted in a variable-temperature static exchange-gas cryostat. Optical excitation is provided by a 1 W TEM_{00} Nd/YAG (yttrium aluminum garnet) laser ($\lambda = 1064$ nm). Neutral density filters and three different spot sizes (1.9×10^{-4}, 8.8×10^{-4}, and 1.8×10^{-3} cm^{-2}) are used to probe a wide range of injection conditions. Photoluminescence is collected by CaF_2 optics and analyzed by a Fourier transform infrared (FTIR) spectrometer. The spectrometer is equipped with a thermoelectrically cooled HgCdZnTe detector, which has a relatively flat response from 0.2 to 1.0 eV.

PL spectra for the nominally LM ($x=0.53$) and nearly LM ($x=0.60$) epistructures at $T=77$ K are shown in Fig. 1. B-B PL at 0.806 and 0.741 eV is very strong, demonstrating the superior quality of these structures. Previously, we measured a peak external radiative efficiency of 63% at room temperature from a similar LM structure, which incorporated an integral parabolic reflector to reduce the trapping of emitted photons.[7] Subsequent work indicated that the internal quantum efficiency is close to 100% at 77 K and that our lattice-mismatched epistructures have comparable efficiency at this temperature, although the emission is more readily thermally quenched by Auger recombination in the lower-band-gap alloys.[4] Returning to Fig. 1, we see that the B-B peak shifts to lower energy with increasing indium concentration as expected. More importantly for the purpose of this work, an additional peak (labeled SBG) is observed at approximately 0.522 eV, more than 0.2 eV below the B-B PL. This level is approximately twice as deep as the defect-related states that are typically reported for this system.[6] Under moderate excitation, the peak has a Gaussian line shape with a full width at halfmaximum of approximately 40 meV, which is much broader than the thermal energy $kT \approx 7$ meV. The SBG peak loses intensity with increasing in-

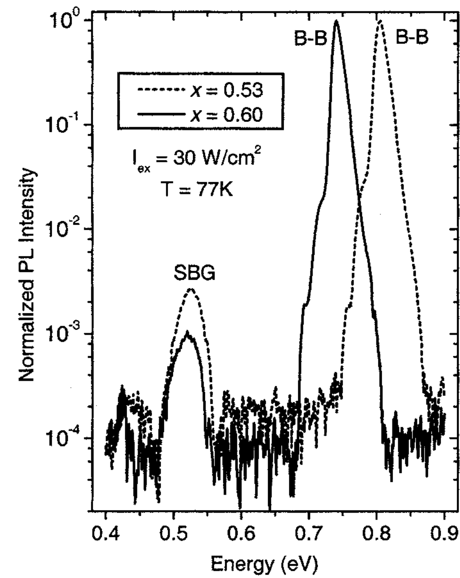

FIG. 1. PL spectra of the LM ($x=0.53$) and nearly LM ($x=0.60$) epistructures at 77 K. The spectra are plotted on a logarithmic vertical scale to highlight weak, sub-band-gap features.

dium concentration and is not observed in the severely mismatched, low-band-gap epistructures (see Fig. 2).

Interestingly, the SBG PL shows no sign of saturation relative to the B-B emission as the excitation is increased to powers up to and exceeding 1000 W/cm^2, where the photoexcited carrier density exceeds 10^{17} cm^{-3}. Indeed, as shown in Fig. 3 and 4, the SBG peak blueshifts and gains strength relative to the B-B emission with increasing excitation for 78 K $\leq T \leq$ 120 K. The results in Fig. 4 follow the relationship $I_{PL} = C I_{ex}^s$, where I_{PL} is the integrated PL intensity, I_{ex} is the excitation density, and C is a constant. In the nearly LM epistructure, we find $s_{avg} = 1.02 \pm 0.01$ for the B-B PL and $s_{avg} = 1.35 \pm 0.01$ for the SBG PL. For this analysis, the SBG PL integral includes the high-energy shoulder that emerges at

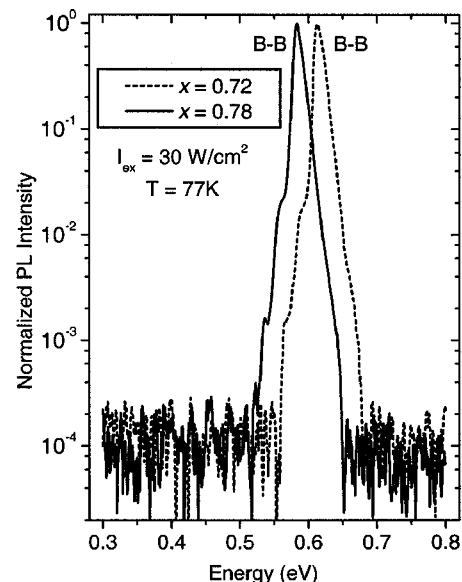

FIG. 2. PL spectra of two severely mismatched, indium-rich epistructures at 77 K. The sub-band-gap peaks that are observed in the less mismatched structures are not present in this case.

Downloaded 07 Nov 2005 to 152.42.169.207. Redistribution subject to AIP license or copyright, see http://jap.aip.org/jap/copyright.jsp

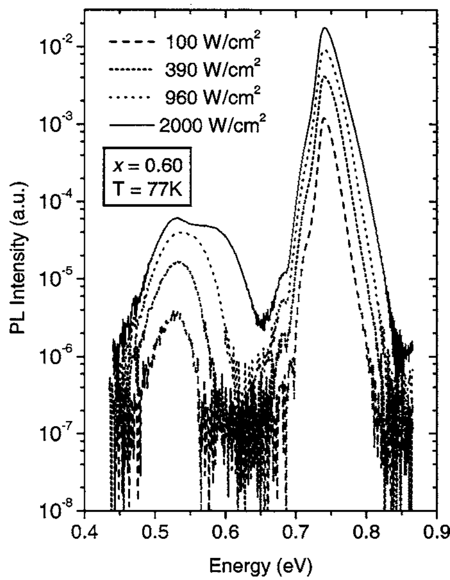

FIG. 3. Photoexcitation dependent PL spectra for the nearly LM epistructure. The spectra from the LM structure show a similar trend.

the highest excitations. We obtain similar results ($s_{avg} = 1.01 \pm 0.01$ for B-B and $s_{avg} = 1.32 \pm 0.03$ for SBG PL) in the LM epistructure, indicating that the SBG features in the LM and slightly mismatched structures are closely related. However, we note that the superlinear excitation-dependent growth of the SBG PL is absent at $T = 4$ K. At this temperature, both peaks (SBG and B-B) increase approximately linearly ($s \approx 1$) with photoexcitation.

In order to further elucidate the recombination mechanism responsible for the SBG PL, we have measured the integrated intensity of the peak as a function of temperature. An Arrhenius plot of this measurement is shown in Fig. 5 for $77 \text{ K} \leq T \leq 187$ K (the emission is too weak to discern at higher temperatures). The temperature dependence yields an activation energy of 25 meV for the LM epistructure and 30

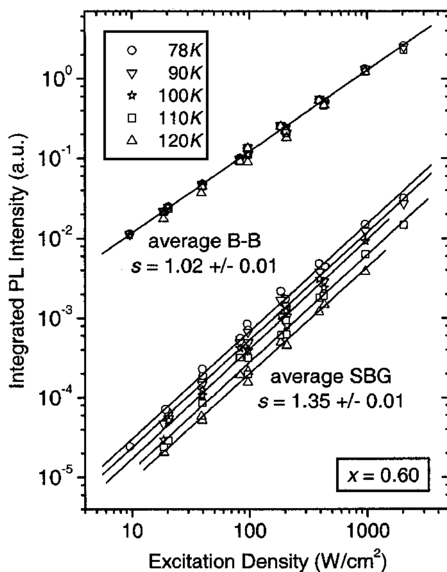

FIG. 4. Integrated PL intensity vs excitation density for the nearly LM B-B and SBG peaks. While the B-B PL grows linearly with excitation as expected, the SBG emission grows more rapidly.

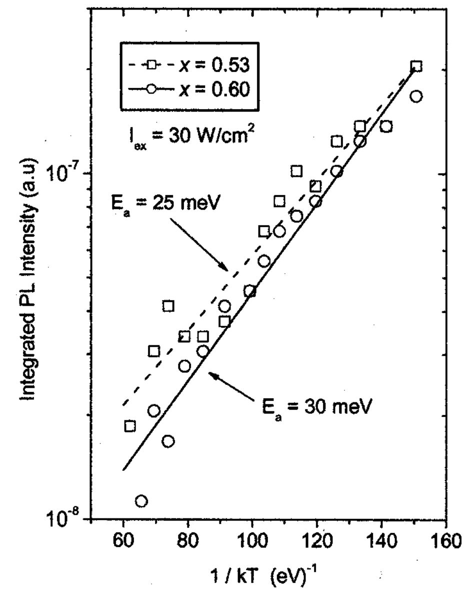

FIG. 5. Arrhenius plot of the integrated SBG PL intensity in the LM ($x = 0.53$) and nearly LM ($x = 0.60$) epistructures. The measured activation energies E_a are indicated on the plot.

meV for the nearly LM epistructure. The congruent behavior in the two systems provides further evidence that the SBG peaks have a common origin. The systematic PL reduction with increasing temperature demonstrates that the excitation-dependent PL enhancement is not a thermal phenomenon. Indeed, the B-B peak position and Boltzmann tail confirm that local heating is relatively small, with $\Delta T \approx 10$ K at the highest excitation levels.

III. DISCUSSION

The observation of a deep level in the LM epistructure that abates in the nearly LM structure and does not appear in the severely mismatched structures supports our previous suggestion that the density of deep states is reduced with increasing mismatch in this system. On the other hand, our SBG PL measurements do not reveal the increasing density of shallow states that were also predicted by that model.[3,4] In this analysis it is important to note that, while PL spectroscopy is a very sensitive probe of radiative levels, the technique cannot detect states that couple weakly with light. Hence, we are currently employing a complementary temperature-dependent transient capacitance technique to investigate the nonradiative centers that may elude the present PL study.

Broad, deep spectral features such as those observed in Fig. 1 are usually attributed to defects. With the exception of some donor-to-acceptor transitions, impurities tend to produce relatively sharp spectral features. In contrast, defect levels depend strongly on the local bonding configuration, which can vary considerably from site to site. This variation produces a broad distribution of energy levels. On the other hand, defect-related recombination typically saturates at high carrier density due to the finite number of defect sites. And our previous radiative efficiency measurements have shown[4] that defect-related transitions are negligible compared to radiative B-B recombination when $I_{ex} > 10 \text{ W/cm}^2$ and the

Downloaded 07 Nov 2005 to 152.42.169.207. Redistribution subject to AIP license or copyright, see http://jap.aip.org/jap/copyright.jsp

photoexcited carrier density exceeds approximately 10^{16} cm^{-3}. The linear growth ($s \approx 1$) of the B-B PL over a relatively wide range of excitation and temperature is consistent with the assumption that we are generally probing a system in a regime of high radiative efficiency, where an absorbed photon usually leads to an emitted photon, and confirms the validity of our measurements. If the radiative mechanism were competing with a rapid nonradiative mechanism, temperature-independent unity slopes would only occur in the unlikely event that the rate of the two mechanisms had the same temperature and excitation dependence.

If the SBG emission obeyed ordinary Shockley-Read-Hall (SRH) statistics,[8] the defect-related recombination rate would vary linearly with the photoexcited carrier density n. Since the B-B radiative rate is proportional to n^2, we would expect the SBG PL to scale sublinearly against B-B PL in this regime. In this context, the uniform, superlinear growth of the SBG PL with excitation is difficult to explain. If we consider the existence of a nonradiative recombination mechanism at the defect sites, the superlinear behavior could be attributed to competition between radiative and nonradiative channels, with the excitation-dependent radiative rate increasing more rapidly than the nonradiative rate. However, the total gain associated with this competition is limited and would only manifest itself over a limited excitation range. Near the limits, the log-log plots shown in Fig. 4 would return to unity slope. In contrast, we see no deviation from uniform, superlinear slope.

The blueshift of the SBG peak (see Fig. 3) with increasing excitation is also inconsistent with SRH statistics as applied to diffuse deep levels at low temperatures. Once a mobile carrier is trapped in such a deep state, it does not have sufficient thermal energy to escape and seek a lower level. In addition, defect sites are presumably sufficiently diffuse to preclude intersite tunneling. Hence, the sequential filling of higher-energy states is not possible. If a thin, low-band-gap alloy layer existed near one of the DH interfaces, carriers in this layer would probably have sufficient mobility to find the lowest available states. Low-band-gap alloy candidates include strained InAsP,[9] where type-II band alignment relative to the bulk InGaAs layer might also occur, and In-rich InGaAs,[10] which would be type II only for light holes. However, high-resolution transmission electron microscopy has established that our growth reactor creates nearly atomically abrupt ($\Delta x < 1$ nm) interfaces.[11] Hence, we consider a different model to explain our unusual results.

IV. PROPOSED MODEL

SBG PL that blueshifts with increasing excitation suggests that donor-acceptor pair (DAP) recombination may be responsible. The DAP transition energy is given by

$$h\upsilon = E_G - E_D - E_A + ke^2/\varepsilon r, \tag{1}$$

where E_G is the band gap, E_D and E_A are the donor and acceptor ionization energies, and $ke^2/\varepsilon r$ is the Coulomb interaction of the DAP.[12] With increasing photoexcited carrier density, the average distance r_{avg} between excited donors and acceptors decreases, yielding an increase in the DAP Coulomb energy. Moreover, since the recombination probability depends on the overlap of the electron and hole wave functions, the DAP recombination rate varies with pair separation r as[13]

$$\omega_{DAP}(r) = \omega_0 e^{-2r/a_B}, \tag{2}$$

where a_B is Bohr radius of the shallower impurity. The exponential increase in the DAP recombination rate with decreasing r may explain the superlinear excitation dependence of the SBG PL.

In order to test this model, we need to estimate the average distance between excited donors and acceptors. The carrier generation rate is $\Omega_{gen}=I_{ex}/(E_{ex}V)$, where I_{ex} is the intensity of the absorbed laser light, E_{ex} is the laser energy ($\lambda = 1064$ nm), and V is the photoexcited volume. Since we are operating in a regime where B-B radiative recombination is dominant, the recombination rate is approximately $\Omega_{rad} = Bn^2/N$, where B is the radiative coefficient and N is the photon recycling factor. We estimate[4] that $N=4$ and, at $T = 77$ K, we calculate[4] $B=3.2\times10^{-10}$ cm^3/s in the nominally LM InGaAs and $B=2.7\times10^{-10}$ cm^3/s in the lower band gap nearly LM alloy. As discussed in Ref. 4, B values are obtained by adjusting the room-temperature LM experimental result[7] ($B=1.5\times10^{-10}$ cm^3/s) according to $B \propto E_G^2/(kT)^{3/2}$, where PL spectra are used to estimate E_G. In steady state, the rate of electron-hole pair generation equals the rate of recombination: $\Omega_{gen}=\Omega_{rad}$. Hence, we can use the excitation intensity I_{ex} to evaluate the steady-state photoexcited carrier density

$$n = \sqrt{NI_{ex}/(BE_{ex}V)}. \tag{3}$$

Next, we use n to estimate the average distance between excited donors and acceptors. The average distance between photoexcited carriers is $d=n^{-1/3}$, giving each carrier a "sphere of influence" with radius $d/2$. Let this sphere be centered on a trap. If a trapped carrier of the opposite sign exists somewhere in this spherical volume, it will have an average distance of $r_{avg}=2^{-1/3}d/2$ from the center. We use this distance to model our experimental results. For each spectrum we fit the SBG peak to a Gaussian profile. Excluding the highest excitations where an asymmetric high-energy shoulder complicates the analysis (see Sec. V below), we obtain very good fits. In Fig. 6, we plot the Gaussian peak center against the average DAP distance r_{avg} described above. We note that, for each individual laser spot size, the peak shifts systematically to higher energy with increasing excitation. The large amount of scatter in the data is primarily due to the variation and uncertainty in spot size. The solid curve is a fit to the data according to Eq. (1): $h\upsilon=E_0 + kq^2/\varepsilon r_{avg}$ with $E_0=E_G-E_D-E_A=0.514$ eV. The fit is excellent, especially in view of the fact that E_0 is the *only* adjustable parameter. To emphasize the extreme sensitivity of the model, the inset graph shows the best fit when we neglect the factor of $2^{-1/3}$ correction noted above.

In Fig. 7, we plot the integrated SBG PL intensity against r_{avg}. Assuming that the measured PL intensity is proportional to the SBG recombination rate, we fit the results to Eq. (2) and obtain the solid and dashed lines shown. Clearly,

Downloaded 07 Nov 2005 to 152.42.169.207. Redistribution subject to AIP license or copyright, see http://jap.aip.org/jap/copyright.jsp

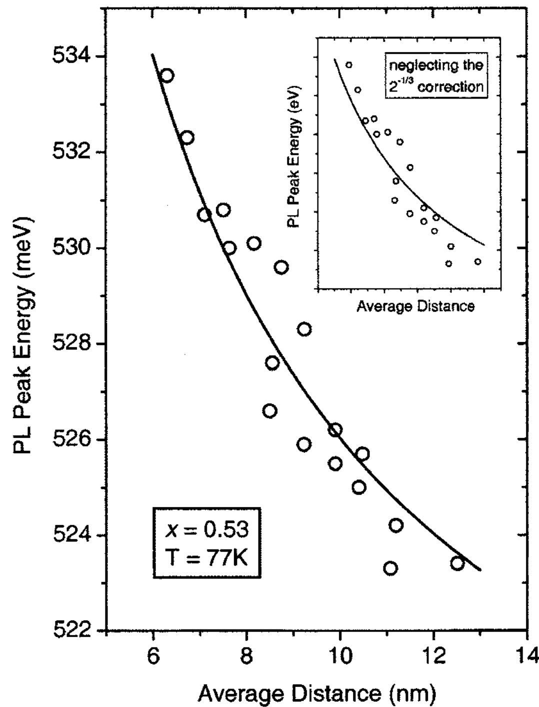

FIG. 6. Gaussian center of the LM SBG peak vs the calculated average DAP distance. The solid curve is the prediction of the DAP model. The inset graph shows the loss of agreement when a relatively minor factor of $2^{-1/3}$ average distance correction is omitted.

the functional form of the DAP model is consistent with our excitation intensity-dependent results. The analysis yields a_B=2.3 nm for x=0.53 and a_B=2.0 nm for x=0.60. With effective masses $m_h^*=0.46m_0$ and $m_e^*=0.04m_0$, these values are close to the acceptor Bohr radius of 1.4 nm (and do not agree with the donor radius of 16 nm) in the host material ($\varepsilon \approx 12$), indicating that the participating acceptor is the shallower trap. Using the average measured value of a_B =2.2 nm, we calculate E_A=39 meV. Then, with the measured band-gap energies E_G=0.803 eV for x=0.53 and E_G =0.738 eV for x=0.60, we obtain deep donor energies E_D =0.250 eV in the LM and E_D=0.185 eV in the nearly LM material.

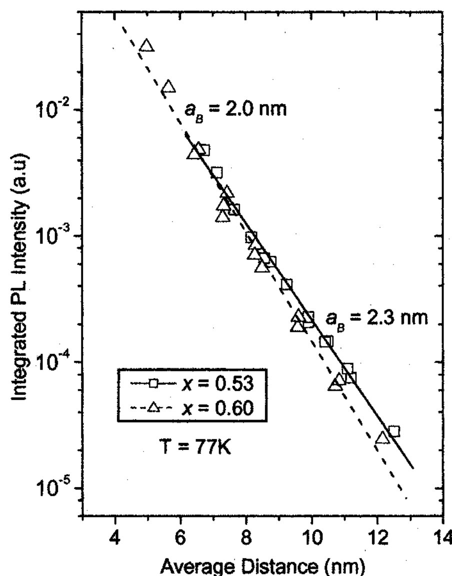

FIG. 7. Integrated PL intensity vs the calculated average DAP distance. In the DAP model, the slope of this plot equals $-2/a_B$, where a_B is Bohr radius of the shallower DAP impurity.

While the relatively short model DAP separations conform with the small value of a_B, the DAP distances still seem extraordinarily short in the context of our high-purity, nominally undoped InGaAs alloys, where we would expect both traps to be relatively dilute ($<10^{15}$ cm^{-3}). Perhaps the close proximity suggested by our analysis can be attributed to the exponential dependence of the transition probability on distance. Distant pairs have a small wave-function overlap so DAP transitions are slow and saturate easily, while transitions involving the more sparse close pairs are rapid and unsaturated, so they dominate the SBG PL signal.

V. FURTHER DISCUSSION

At the highest excitations studied ($I_{ex} > 1000$ W/cm^2), the SBG PL spectrum deviates from a Gaussian profile and a distinct, high-energy shoulder appears (see Fig. 3), indicating that this DAP transition is finally saturating. The high carrier density ($n > 2\times10^{17}$ cm^{-3}) required to saturate this mechanism suggests that the transition rate is indeed rapid and/or the capture cross-section of the deep state is very small. Under these circumstances, the DAPs could be dilute as expected, but would also be difficult to fill and saturate. Fitting the high-excitation spectrum to two Gaussians, we find that the high-energy SBG peak lies approximately 50±5 meV above the low-energy peak. The double Gaussian fit also suggests that the lower-energy peak shifts back to the red under these excitation conditions. The higher-energy peak could be related to transitions between deep donor electrons and valence-band free holes, or DAP transitions involving an acceptor and an excited deep donor level. Let us assume the latter: that the emerging higher-energy peak is associated with the presence of a second electron in an excited state at certain deep donor sites. Since these doubly occupied sites would be relatively sparse, they would be associated with the more widely separated, lower-energy DAP transitions. In this case, the apparent redshift of the low-energy peak could be attributed to the rise in the intensity of these transitions relative to the blueshifted transitions of closer DAPs. The PL enhancement itself would result from the higher occupation probability of the ground state at these sites or an augmented transition rate due to the increased DAP Coulomb interaction.

We also note that as the indium concentration is increased from x=0.53 to x=0.60, and the $In_xGa_{1-x}As$ band gap decreases by approximately 65 meV, the energy of the SBG PL only falls by about 5 meV. Theoretically, the change in E_G with x is primarily due to a shift in the conduction band edge—the valence-band energy is predicted to be nearly independent of alloy composition in bulk InGaAs.[14] These band offset calculations reinforce our assignment of the deep level to an electron trap. With the energy of the highly localized, deep donorlike level effectively fixed, the DAP transition energy should be nearly independent of x.

Our temperature-dependent observations are consistent

Downloaded 07 Nov 2005 to 152.42.169.207. Redistribution subject to AIP license or copyright, see http://jap.aip.org/jap/copyright.jsp

with the DAP model. The absence of superlinear behavior at $T=4$ K can be attributed to the prevalence of excitons at this temperature. Since the exciton binding energy in $In_{0.53}Ga_{0.47}As$ is approximately 2 meV,[15] excitons are the dominant species at 4 K ($kT=0.3$ meV), while free carriers are more numerous for $T\geq 77$ K ($kT=7$ meV). This distinction dictates fundamental changes in the trapping and recombination statistics, which are manifested in the excitation-dependent behavior. At 4 K we expect trapping of excitons rather than free carriers, so the SBG transitions may involve deep donor-bound excitons such as those observed in high-purity n-type InP.[16] The electron-hole separation would be independent of carrier concentration for excitonic SBG recombination and the rate would scale linearly with that of B-B free excitons. We note that a shift from superlinear excitation dependence ($s=1.33$) at $T=40$ K to nearly linear behavior ($s=1.07$) at $T=2$ K has also been observed in $Al_{0.48}In_{0.52}As$ SBG PL.[17] However, those authors attribute the increase in s with T to a different mechanism: the thermally activated changeover from bound-to-bound (i.e., DAP) to free-to-bound (i.e., conduction band to neutral acceptor) transitions.

Finally, we propose two possible explanations for the thermal quenching of the SBG PL with increasing temperature. The 25-30 meV activation energy is close to the acceptor ionization energy $E_A=39$ meV determined above. Hence, the decrease in DAP recombination with increasing temperature may be due to the decreasing thermal occupation of acceptor states. Meanwhile, we note that the measured activation energy is comparable to the energy of optical phonons in InGaAs ($h\upsilon\approx 30$ meV),[18] pointing to the possibility of phonon-mediated nonradiative transitions between the levels involved.

VI. CONCLUSION

We have used FTIR PL analysis to extend our investigation of high-quality LM $In_xGa_{1-x}As/InAs_yP_{1-y}$ double heterostructures grown on InP substrates. As x increases, the buffer between the substrate and the DH accommodates increasingly severe lattice mismatch with surprisingly low defect-related recombination rates in the active layer. We continue to identify the physical and electrical attributes of defects in this system that lead to this highly desirable behavior. By measuring PL spectra down to 0.3 eV over a wide range of photoexcitation and temperature, we verify that radiative deep levels are present in the less mismatched epistructures and that the number and/or optical activity of these levels is reduced with increased mismatch. Since deep levels can impair device performance by providing effective trapping and/or recombination centers, the apparent elimination of these levels with increasing mismatch may help to explain the extraordinary performance of our lattice-mismatched devices.[2]

Excitation-dependent PL measurements are analyzed in the context of a DAP recombination model. This analysis indicates that the SBG peaks observed in the PL spectra of the LM and nearly LM epistructures are related to deep ($E_D=0.250$ eV for $x=0.53$ and $E_D=0.185$ eV for $x=0.60$) donorlike levels. The energy levels are nearly independent of alloy composition, with the change in ionization energy being primarily due to the shifting conduction band edge. Our analysis also suggests that the deep donorlike traps provide for rapid DAP transitions only when an acceptor is extraordinarily close ($r\approx 10$ nm). The direct observation of deep levels in $In_{0.53}Ga_{0.47}As$ and their disappearance with increasing x give credence to our previous defect-related DOS analysis,[3] with the caveat that additional nonradiative states may also be present. Complementary transport measurements that are sensitive to such nonradiative traps are now underway.

The authors would like to thank J. J. Carapella for performing the MOVPE growth, with support from Bechtel Bettis, Inc., and Dr. Wyatt Metzger and Dr. Yong Zhang for helpful discussions. Acknowledgement is made to the donors of The Petroleum Research Fund, administered by the American Chemical Society, for support of this work.

[1] R. K. Ahrenkiel, S. W. Johnston, J. D. Webb, L. M. Gedvilas, J. J. Carapella, and M. W. Wanlass, Appl. Phys. Lett. **78**, 1092 (2001).
[2] M. W. Wanlass, S. P. Ahrenkiel, R. K. Ahrenkiel, J. J. Carapella, R. J. Wehrer, and B. Wernsman, AIP Conf. Proc. **738**, 427 (2004).
[3] T. H. Gfroerer, L. P. Priestley, F. E. Weindruch, and M. W. Wanlass, Appl. Phys. Lett. **80**, 4570 (2002).
[4] T. H. Gfroerer, L. P. Priestley, M. F. Fairley, and M. W. Wanlass, J. Appl. Phys. **94**, 1738 (2003).
[5] T. Yagi, Y. Fujiwara, T. Nishino, and Y. Hamakawa, Jpn. J. Appl. Phys., Part 2 **22**, L467 (1983).
[6] F. R. Bacher, J. Appl. Phys. **64**, 708 (1988).
[7] T. H. Gfroerer, E. A. Cornell, and M. W. Wanlass, J. Appl. Phys. **84**, 5360 (1998).
[8] W. Shockley and W. T. Read, Jr., Phys. Rev. **87**, 835 (1952); R. N. Hall, *ibid.* **87**, 387 (1952).
[9] S. K. Haywood, A. C. H. Lim, R. Gupta, S. Emery, J. H. C. Hogg, V. Hewer, M. Hopkinson, and G. Hill, J. Appl. Phys. **94**, 3222 (2003).
[10] C. Lugand, T. Benyattou, G. Guillot, T. Venet, M. Gendry, G. Hollinger, and B. Sermage, Appl. Phys. Lett. **70**, 3257 (1997).
[11] S. P. Ahrenkiel and M. W. Wanlass (unpublished).
[12] J. J. Hopfield, D. G. Thomas, and M. Gershenzon, Phys. Rev. Lett. **10**, 162 (1963).
[13] D. G. Thomas, J. J. Hopfield, and W. M. Augustiniak, Phys. Rev. **140**, A202 (1965).
[14] K. Kim, G. L. W. Hart, and A. Zunger, Appl. Phys. Lett. **80**, 3105 (2002).
[15] S. Adachi, *Physical Properties of III–V Semiconductor Compounds* (Wiley, New York, 1992), p. 157.
[16] R. Benzaquen, S. Charbonneau, R. Leonelli, and A. P. Roth, Phys. Rev. B **53**, 3627 (1996).
[17] H. P. Zhou and C. M. S. Torres, J. Appl. Phys. **75**, 3571 (1994).
[18] S. Adachi, in *Properties of Lattice-Matched and Strained Indium Gallium Arsenide*, edited by P. Bhattacharya (INSPEC, London, 1993), p. 47.

Downloaded 07 Nov 2005 to 152.42.169.207. Redistribution subject to AIP license or copyright, see http://jap.aip.org/jap/copyright.jsp